Speed dependence of collisional relaxation in ground vibrational state of OCS: Rotational behaviour

Maxim A. Koshelev, Mikhail Yu. Tretyakov, François Rohart, and Jean-Pierre Bouanich

Citation: J. Chem. Phys. **136**, 124316 (2012); doi: 10.1063/1.3696895
View online: http://dx.doi.org/10.1063/1.3696895
View Table of Contents: http://jcp.aip.org/resource/1/JCPSA6/v136/i12
Published by the American Institute of Physics.

Speed dependence of collisional relaxation in ground vibrational state of OCS: Rotational behaviour

Maxim A. Koshelev,[1] Mikhail Yu. Tretyakov,[1,a)] François Rohart,[2] and Jean-Pierre Bouanich[3]
[1]*Institute of Applied Physics of the Russian Academy of Sciences, 46 Ulyanov str., Nizhny Novgorod 603950, Russia*
[2]*Laboratoire de Physique des Lasers, Atomes et Molécules, UMR CNRS 8523, Université de Lille 1, 59655 Villeneuve d'Ascq Cedex, France*
[3]*Institut des Sciences Moléculaires d'Orsay UMR 8214, CNRS-Université Paris Sud, 91405 Orsay Cedex, France*

(Received 28 December 2011; accepted 2 March 2012; published online 30 March 2012)

Accurate experimental data on pressure broadened profiles of $^{16}O^{12}C^{32}S$ pure rotational lines in a broad range of quantum number J have been analyzed taking into account the speed dependence of collisional relaxation. Refined values of collisional self-broadening coefficients are determined and compared to previously known data. New quantitative information on departures of observed line shapes from the traditional Voigt profile is obtained. It is shown that these departures result mainly from the speed dependence of collisional relaxation. Theoretical calculations of self-broadening parameters are performed in the framework of the semiclassical impact Robert-Bonamy formalism where the mean relative molecular speed as well as the Maxwell-Boltzmann distribution of relative speeds is considered. The necessity of allowance for the speed dependence in line shape models is confirmed and satisfactory results have been obtained by arbitrarily limiting the integration of the differential cross section to a finite value of the impact parameter. It is shown for the first time for the whole rotational spectrum that speed dependent models not only improve accuracy of modeling the observed line profiles but also give physically grounded values of collisional relaxation parameters. © *2012 American Institute of Physics*. [http://dx.doi.org/10.1063/1.3696895]

I. INTRODUCTION

Modern remote sensing instruments demand very high spectroscopic accuracy (see, e.g., ACCURATE mission requirements in Ref. 1). It is well known that in most cases the traditional Voigt model fails to reproduce molecular line absorption profile recorded with a sufficiently high signal to noise ratio achievable nowadays in laboratory studies.[2] A real line is slightly higher and narrower than predicted by the Voigt model. Two principally different physical mechanisms, namely, velocity changing collisions and speed dependence of collisional relaxation, are considered to be responsible for this effect. Under certain conditions, experimental data can be equally well reproduced by a model based on one or another mechanism. However, extensive study of the subject (see the review paper, Ref. 3 and references therein) demonstrates predominant influence of the speed dependence effect on observed line shapes, except for the exotic case of weak collisions.[2] Based on this conclusion the speed dependent Voigt profile is suggested as the actual line shape model to be used.

To the best of our knowledge, there are no publications presenting analysis of the speed dependence effects observed in experiment and supported by theoretical calculations in a broad range of rotational quantum number. In this paper, the speed dependent Voigt model was used for the line shape analysis in a well resolved pure rotational spectrum of carbonyl sulfide (OCS) at pressures up to a few Torr. The studied lines correspond to quantum numbers J ranging from 1 to 69, covering the largest part of the rotational spectrum observable at room temperature. Experimental recordings of the $^{16}O^{12}C^{32}S$ spectrum lines were obtained in 24–850 GHz frequency range employing a spectrometer with radio-acoustic detection of absorption (the RAD spectrometer).[4] Analysis of the shape of these lines using conventional Lorentz and Voigt profiles was reported earlier.[5] The analysis revealed perfect linear dependence of the collisional relaxation parameter on pressure for all observed transitions and its smooth dependence on J demonstrating high quality of the experimental data. However, minor systematic deviations observed in the fit residuals (see, e.g., Fig. 1 in Ref. 5) show that the used model is not fully adequate and further thorough analysis of observed line shapes is required. Results of such an analysis are reported in this paper. For reader's convenience, details of the experiment and specificities of the data are shortly reviewed in Sec. II. Analysis of the observed line shapes is given in Sec. III by considering various profile models. Theoretical self-broadening coefficients of OCS rotational lines calculated using the semiclassical Robert-Bonamy (RB) formalism[6] are reported in Sec. IV. The intermolecular potential used includes a dispersion energy contribution in addition to the overwhelming electrostatic interactions, involving dipole, quadrupole,

a)Author to whom correspondence should be addressed. Electronic mail: trt@appl.sci-nnov.ru.

and octopole contributions. The calculations have been performed for the mean relative molecular speed and by considering the Maxwell-Boltzmann distribution of relative speeds.

II. EXPERIMENTAL DETAILS

Detailed description of the RAD spectrometer used for the study and the method of measurement can be found in Ref. 4 and references therein. The radiation source (Backward Wave Oscillator – BWO) is phase-locked against the harmonic of the reference synthesizer of either 8–18 GHz or 78–118 GHz operating frequency range synchronized with rubidium frequency standard signal. Line recording is realized via step-by-step frequency scan of the reference synthesizer. Use of the high-stable radiation source, amplitude modulation of radiation beam, and synchronous detection of the absorption signal allow recording the true line shape with signal-to-noise ratio better than 1000.

The gas cell is a well polished copper tube, two centimeters in diameter with an optical path length ℓ varying from 0.5 to 10 cm, thus providing the small optical path length condition necessary for proper registration of absorption signal by the spectrometer (see Ref. 4 for more details). A high-sensitive membrane microphone coupled with the cell converts the acoustic wave into the electric signal. The cell is permanently connected to a vacuum system as well as vacuum pumps, gas sample, and pressure gauge (MKS Baratron type 627 with declared accuracy of 0.12%).

In the course of the experiment, the gas cell was filled with an OCS sample up to a maximum pressure and the absorption spectrum in the vicinity of the studied line was recorded. The maximum OCS pressure was 3–4 Torr for high-J lines, while for low-J lines the pressure did not exceed 1.2–1.5 Torr to avoid overlapping of the rotational lines of ground and v_2 excited vibrational states (see Fig. 1). Then, the cell was stepwise evacuated and spectrum recording was performed for eight to ten different pressures. Line recordings at each pressure were repeated a few times to estimate statistical uncertainty of the measurement.

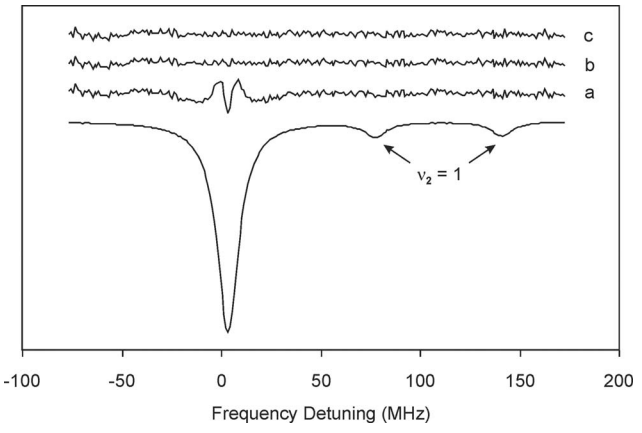

FIG. 1. $J \rightarrow J' = 4 \rightarrow 5$ line of OCS. Residuals (obs.-cal., amplified by 20) correspond to Voigt (a), Q–SD–Voigt (b), and HG–SD–Voigt (c) profiles. Frequency detuning from 60.810 GHz is shown. Temperature: 299 K. Cell length: 10 cm. OCS pressure: 1.072 Torr. Doppler half-width at 1/e level: 0.058 MHz. Voigt collisional half-width: 6.557(5) MHz. Calculated peak relative absorption at infinite pressure: 0.75%. The weak neighboring lines correspond to a rotational doublet of the $v_2 = 1$ excited vibrational state.

The length of the gas cell was adjusted to the absorption coefficient of the studied line, whose intensity could vary up to three orders of magnitude. For recording OCS lines in the vicinity of $J = 40$ (corresponding to the most intense lines) the cell length was as short as 0.5 cm, providing optical depth less than 10^{-1}. To keep satisfactory sensitivity of the acoustic cell for studying less intensive lines, the cell length was gradually increased up to 10 cm, maintaining optical depth less than 10^{-1} for minimizing the line shape distortion. The test measurement of the $J \rightarrow J' = 58 \rightarrow 59$ line parameters was performed at two radiation path lengths (0.5 and 1.5 cm) and revealed a good agreement of the measured line widths within experimental uncertainties (see Fig. 2 in Ref. 5). It proves that line distortions due to large optical depths are negligibly small in our experiments and the results on line widths do not include the corresponding systematic error. Nevertheless, for an accurate line shape analysis the Beer-Lambert law was taken into account systematically (see Sec. III B).

III. LINE SHAPE ANALYSIS

A. Line shape models

Several line shape models have been considered in this work for experimental data analysis, beginning with the well-known Voigt profile. The latter is obtained from a convolution of a Lorentzian profile related to collisional relaxation and having $\Delta\nu$ half-width at half-maximum (HWHM), and of a Gaussian one related to the Doppler effect due to molecular velocities and having $k v_{a0}/(2\pi)$ half-width at 1/e level of the profile amplitude, where $k = 2\pi\nu_0/c$ is wavenumber (ν_0 is line frequency, c is light speed) and v_{a0} is the most probable absorber speed. Since this model neglects correlations between molecular velocities and frequency of collisions, more sophisticated profiles are required.

Molecular collisional relaxation rate Γ is a characteristic of decay of the optical coherence induced between lower and upper states of the corresponding molecular transition. This rate is directly linked to the coherence relaxation time $\tau = 1/\Gamma$ in the time domain or to the collisional width $\Delta\nu = \Gamma/(2\pi)$ in the frequency domain.

On the one hand, Γ depends on the relative speed v_r of collisional partners. This results in the dependence of Γ on absorber speed v_a. The effect is stronger for a larger ratio of buffer to absorber molecule mass $\lambda = m_b/m_a$. The line shape is then described by a speed dependent (SD) Voigt profile. Since relaxation rates are larger for higher relative speeds, SD-Voigt profiles are narrower than the corresponding Voigt profile. Two SD-Voigt profiles have been considered:

(1) The hypergeometric model[7,8] (hereafter HG-SD-Voigt model) which assumes an effective collisional interaction potential of the form $V(r) \propto 1/r^q$ where r is the intermolecular distance. The dependence of the relaxation rate on the relative speed takes the form $\Gamma(v_r) \propto v_r^\alpha$ with $\alpha = (q-3)/(q-1)$. Introducing the average rate $\Gamma_0 = \langle\Gamma(v_r)\rangle_{vr}$ and taking into account that $\langle\Gamma(v_r)\rangle_{vr}$

$= \langle \Gamma(v_a) \rangle_{va}$,[9,10] the speed dependence of the collisional relaxation rate on the absorber speed is written as

$$\Gamma(v_a) = \frac{\Gamma_0}{(1+\lambda)^{\alpha/2}} \mathrm{M}\left[-\frac{\alpha}{2}; \frac{3}{2}; -\lambda\left(\frac{v_a}{v_{a0}}\right)^2\right], \quad (1)$$

where $\mathrm{M}(a;\ b;\ x)$ is the confluent hypergeometric function.[11]

(2) The quadratic model[12] (hereafter Q-SD-Voigt model) in which $\Gamma(v_a)$ takes the form

$$\Gamma(v_a) = \Gamma_0 + \Gamma_2\left[\left(\frac{v_a}{v_{a0}}\right)^2 - \frac{3}{2}\right], \quad (2)$$

where Γ_2 is the parameter describing the speed dependence of the collisional relaxation rate. In addition to its simpler form leading to faster numerical calculations, this quadratic model is useful because, by contrast to parameter α, Γ_2 is pressure dependent, which allows a simple test for the relevance of speed dependence.[13]

These two models can be coupled via the approximated relation[10,14]

$$\frac{\Gamma_2}{\Gamma_0} = \frac{\alpha\,\lambda}{3(1+\lambda)^{\alpha/2}} \mathrm{M}\left[1 - \frac{\alpha}{2}; \frac{5}{2}; -\frac{3}{2}\lambda\right]. \quad (3)$$

On the other hand, collisions are responsible for absorber velocity changes. The corresponding molecular confinement or diffusion process results in reduction of the Doppler effect, leading to line narrowing (Dicke effect).[15] This effect is more pronounced as the collisional relaxation is weaker. It is usually described either by the Galatry profile in the case of the soft collision model,[16] or by the Rautian profile in the case of the hard collision model.[17] In addition to the conventional relaxation rate Γ_0, these two models involve a narrowing parameter β_{opt} also called optical diffusion rate (see, e.g., Refs. 2, 13, and 18). Let us note that these two models are almost equivalent from the point of view of line fitting,[13] so only the Galatry profile has been considered in this work.

Actually, these two processes, speed dependence of collisional relaxation rates and velocity changing collisions, occur simultaneously. Thus, absorption profiles should be described by the SD-Galatry profile[19] or similarly by an SD-Rautian profile. However, as these processes both lead to line narrowing, it is quite difficult to discriminate their relative contributions from the experimental point of view, even when quite large signal to noise ratios are achieved.[20] As a matter of fact, it should be noted that the Dicke effect has an effective influence only in the Doppler regime (i.e., for low pressures when Γ_0 is less or near kv_{a0}), whereas SD-effects occur whatever the gas pressure is. Moreover, the Dicke effect only appears when optical coherences are not completely destroyed by velocity changing collisions. The optical diffusion rate β_{opt} can be viewed as referring solely to molecules suffering significant velocity changes while preserving their optical coherence. This rate differs from the kinetic diffusion rate β_{kin}, which can be deduced from the relation $\beta_{\mathrm{kin}} = k_{\mathrm{B}}T/m_a D_{ab}$ (see Refs. 21 and 22 and references therein), where k_{B} is Boltzmann constant and D_{ab} is the mass diffusion coefficient for a mixture of absorbing and buffer molecules. The corresponding time $(1/\beta_{\mathrm{kin}})$ is the duration after which a molecule forgets its initial velocity. So, several studies[2,10,13,20,23–25] inferred that the molecular relaxation rate Γ_0 should not be too large as compared to the kinetic diffusion rate β_{kin}. Therefore, the optical rate should be smaller than the kinetic one, $\beta_{\mathrm{opt}}/\beta_{\mathrm{kin}}$ tending toward zero when $\Gamma_0/\beta_{\mathrm{kin}}$ is getting larger.

B. Line fits and data analysis

The observed line shapes have been analyzed by using the least-squares fit code developed in Lille[10,13,24] and based on discrete Fourier transform techniques. Indeed, the absorption line shape $S(\nu)$ is the real part of the Fourier transform of the polarization correlation function $\Phi(t)$, that is the time domain absorber response at resonant pulse excitation.[12,26] This method is particularly interesting because, in the case of Voigt, SD-Voigt, Galatry, and SD-Galatry profiles, analytical expressions are available for $\Phi(t)$.[10,19] So, the accuracy on theoretical line shapes can be set as high as wanted just by increasing the number of points considered in the discrete Fourier transform.

Some modification of the line shape fitting code was made to take into account the specific features of the spectrometer. Instead of measuring the absolute sample transmission, the acoustic detection scheme registers the signal, which is directly proportional to the power of radiation absorbed by the gas. Thus, the Beer-Lambert law was considered in the theoretical profiles by computing the line intensity I_{if} from data of Ref. 27. For the least-squares routine used in the analysis of line shapes, the Doppler broadening was kept fixed at the calculated value corresponding to the experimental conditions, whereas the adjusted parameters were the central line frequency ν_0, the collisional line width $\Delta\nu$, the signal amplitude A_0 and, if relevant, the speed dependence or diffusion parameters. Finally, some experimental artifacts, namely, slight line asymmetries caused by the residual baseline distortions were modeled by introducing a linear baseline and an extra term proportional to the imaginary part of the Fourier transform of the correlation function $\Phi(\tau)$.

The following model function was fitted to the observed spectra:

$$S(\nu-\nu_0) = A_0 \cdot \exp\left\{-I_{if}\, P\ell\Re e\left[F(\nu-\nu_0)\right]\right\} + a_0 + a_1\cdot(\nu-\nu_0) + a_2\cdot\Im m\left[F(\nu-\nu_0)\right], \quad (4)$$

where $F(\nu)$ is the Fourier transform of the correlation function $\Phi(\tau)$, P is gas pressure, and a_0, a_1, and a_2 are adjustable parameters.

As an example, Fig. 1 displays the results obtained for the $J \rightarrow J' = 4 \rightarrow 5$ line of OCS at 60.814 GHz. This case is typical of low frequency lines for which it is necessary to take into account some extra lines belonging to the thermally populated $\nu_2 = 1$ excited vibrational state. Thanks to the good signal to noise ratio achieved, one observes a clear departure from the usual Voigt profile characteristic of line narrowing, the observed peak amplitude being larger than that of the Voigt profile. A good agreement between the model and the experimental record is obtained by using an SD-Voigt profile.

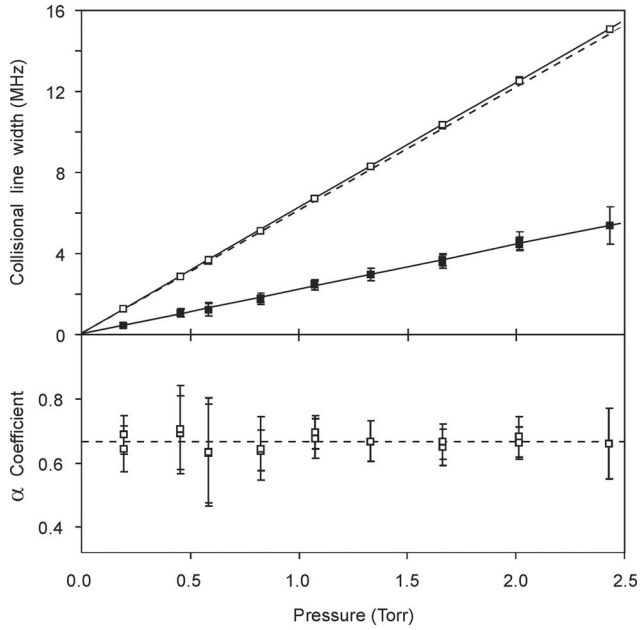

FIG. 2. Collisional self-relaxation of the $J \rightarrow J' = 4 \rightarrow 5$ line of OCS at 60.814 GHz at 299 K. Line shape characteristics derived by different models versus pressure. Straight lines are derived from weighted least squares fits. Error bars correspond to three standard deviations. Upper panel: Voigt [collisional broadening is presented by dashed line fitted to experimental points (not shown): $\gamma_0 = 6.052(3)$ MHz/Torr.]; Q-SD-Voigt [empty squares (error bars are not shown, their sizes are smaller than dimensions of the symbol) and solid line: $\gamma_0 = 6.182(6)$ MHz/Torr, $\gamma_2 = 0.738(9)$ MHz/Torr (for the sake of visibility, the plotted $\Gamma_2/(2\pi)$ experimental values (■) have been multiplied by 3)]. Lower panel: HG-SD-Voigt [α (□): $\langle\alpha\rangle = 0.668(5)$].

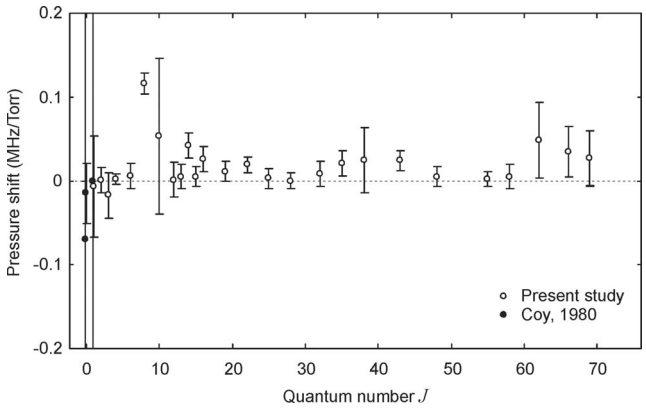

FIG. 3. OCS self-shifting parameters δ_0 (in MHz/Torr) at room temperature versus rotational quantum number J. Experimental values retrieved from Voigt profile fits: this work (empty circles); Coy[14] (filled circles). Error bars correspond to three standard deviations.

Both SD-models (quadratic or hypergeometric) are equivalent, leading to a signal to noise ratio, defined as the line amplitude divided by the residual standard deviation value, larger than 1500. Similar records have been obtained for pressures ranging from 0.4 to 2.4 Torr.

Figure 2 (upper panel) presents the pressure dependence of collisional relaxation rates derived from the Voigt and Q-SD-Voigt profiles. For clarity, the HG-SD-Voigt profile case is not shown here. As expected, these rates vary linearly with the gas pressure P. Y-intercepts of the straight lines fitted to the experimental data can be considered to be zeros within statistical uncertainty of these data. The corresponding pressure broadening γ_0 and speed dependence γ_2 parameters, defined as $\gamma_i = (2\pi)^{-1}\mathrm{d}\Gamma_i/\mathrm{d}P$ for $i = 0$ and 2, were derived by weighted least-squares calculations. Q-SD-Voigt and HG-SD-Voigt models lead to quite similar values of γ_0 (6.182(6) and 6.175(5) MHz/Torr, respectively; one-sigma statistical uncertainty is given here and after in parentheses for the last digit quoted). As expected, they are significantly larger than the parameter related to the Voigt profile (6.052(3) MHz/Torr) because of the line narrowing related to speed dependence processes. On the other hand, the Q-SD-rate Γ_2 varies linearly with pressure, in good agreement with the binary collisional regime occurring in this pressure range. This feature gives a strong evidence of the important contribution of the speed dependence of relaxation rates in the considered pressure range (0.2–2.4 Torr) where collisional broadening is predominant (the collisional HWHM is 1–15 MHz, the Doppler HWHM is 0.049 MHz). The role of the velocity changing collisions (Dike narrowing) is expected to be negligibly weak in this range.

Within the framework of the HG-SD-Voigt model, the SD-parameter α is, as expected, pressure independent within statistical uncertainty with a mean value $\langle\alpha\rangle = 0.668(5)$ (see Fig. 2, lower panel). Within the Berman-Pickett model, this corresponds to an effective interaction potential $V(r) \propto 1/r^q$ with $q = 7.02(9)$. It is interesting to note that, by using Eq. (3), this α-value leads to ratio $\gamma_2/\gamma_0 = 0.125(1)$, in good agreement within three standard deviations with the ratio deduced from the Q-SD-Voigt model fits $\gamma_2/\gamma_0 = 0.119(2)$.

A similar analysis has been performed for 26 absorption lines with J ranging from 1 to 69 within the 24–850 GHz frequency range. The corresponding collisional relaxation parameters retrieved from the Voigt (γ_0), Q-SD-Voigt (γ_0, γ_2), and HG-SD-Voigt (γ_0, α) profiles are listed in Table I. The reported γ_0 and γ_2 values refer to 296 K. They were deduced from retrieved experimental values by using the usual temperature law[28] T^{-n} with n fixed to values given in Ref. 29. The results of the SD analysis are not presented for two lines: (i) for the line with $J = 1$ because the results could be affected by experimental artifacts, as discussed in Sec. III C, and (ii) for the line with $J = 10$ because the signal to noise ratio was insufficient for using SD-Voigt models.

The quoted line frequencies derived from the Voigt profile fits correspond to the values extrapolated to zero-pressure. They are in good agreement with the results of the Lamb-dip study of OCS rotational transitions in mm/submm range,[30] which confirms consistency of our data. The derived values of pressure induced frequency line shifts are plotted in Fig. 3 versus J. Values of the shifts are comparable within their statistical uncertainty because they are quite small. For majority of lines the shifting parameter was found to be positive and smaller than 30 kHz/Torr, in agreement with the results of our previous work.[5] The values obtained are not presented here because careful study of line shifting is beyond the scope of this paper.

Parameters γ_0 derived from the Voigt and HG-SD-Voigt profiles are compared in Fig. 4 (upper panel). As is always the case in self-collisional relaxation, one observes a

TABLE I. Relaxation parameters of $J \rightarrow (J+1)$ rotational lines of $^{16}O^{12}C^{32}S$ related to Voigt, Q-SD-Voigt, and HG-SD-Voigt profiles. The uncertainties (in units of the last digit quoted) refer to one standard deviation. See text for details.

	Frequency	Voigt	Q-SD-Voigt		HG-SD-Voigt		HG-SD-Voigt	
J	ν_0 (MHz)	γ_0 (MHz/Torr)	γ_0 (MHz/Torr)	γ_2 (MHz/Torr)	γ_0 (MHz/Torr)	α	γ_0^{calc} (MHz/Torr)	α^{calc}
1	24325.915 (11)	5.838 (13)	...	...	...	...	6.189	0.820
2	36488.813 (4)	6.020 (6)	6.168 (15)	0.781 (28)	6.158 (14)	0.672 (13)	6.202	0.814
3	48651.625 (8)	6.018 (5)	6.153 (7)	0.733 (19)	6.144 (6)	0.660 (10)	6.227	0.806
4	60814.271 (1)	6.105 (3)	6.236 (6)	0.744 (9)	6.229 (5)	0.668 (5)	6.258	0.797
6	85139.102 (3)	6.191 (7)	6.272 (8)	0.590 (22)	6.269 (8)	0.642 (22)	6.339	0.773
8	109462.989 (5)	6.368 (7)	6.617 (18)	0.933 (49)	6.600 (17)	0.682 (15)	6.437	0.744
10	133785.856 (41)	6.480 (26)	...	...	...	...	6.545	0.713
12	158107.365 (7)	6.509 (10)	6.634 (19)	0.738 (44)	6.627 (18)	0.664 (12)	6.654	0.683
13	170267.491 (4)	6.557 (6)	6.662 (10)	0.679 (26)	6.656 (10)	0.608 (9)	6.707	0.670
14	182427.167 (6)	6.629 (5)	6.703 (16)	0.622 (42)	6.700 (16)	0.580 (10)	6.756	0.657
15	194586.419 (4)	6.669 (5)	6.790 (11)	0.731 (26)	6.783 (10)	0.601 (7)	6.803	0.646
16	206745.144 (5)	6.702 (5)	6.792 (10)	0.654 (34)	6.787 (10)	0.592 (14)	6.845	0.637
19	243218.034 (6)	6.808 (8)	6.984 (27)	0.763 (65)	6.977 (25)	0.634 (13)	6.940	0.617
22	279685.294 (3)	6.822 (4)	6.930 (16)	0.708 (53)	6.924 (15)	0.598 (17)	6.979	0.609
25	316146.092 (4)	6.780 (5)	6.910 (12)	0.692 (30)	6.905 (12)	0.575 (8)	6.958	0.611
28	352599.574 (3)	6.734 (5)	6.852 (15)	0.763 (25)	6.844 (14)	0.598 (8)	6.877	0.621
32	401191.380 (6)	6.574 (4)	6.776 (7)	0.979 (19)	6.762 (7)	0.738 (11)	6.685	0.642
35	437624.524 (4)	6.331 (6)	6.480 (17)	0.846 (40)	6.469 (16)	0.642 (19)	6.488	0.662
38	474047.578 (16)	6.126 (11)	6.325 (20)	0.903 (62)	6.305 (20)	0.698 (20)	6.259	0.682
43	534727.771 (6)	5.731 (5)	5.936 (17)	0.941 (39)	5.920 (16)	0.774 (20)	5.833	0.712
48	595373.626 (4)	5.310 (6)	5.449 (9)	0.692 (20)	5.442 (9)	0.691 (6)	5.391	0.732
55	680212.618 (4)	4.867 (4)	5.023 (18)	0.764 (55)	5.012 (17)	0.738 (24)	4.813	0.730
58	716546.539 (7)	4.693 (3)	4.842 (11)	0.728 (22)	4.832 (11)	0.711 (15)	4.593	0.717
62	764965.996 (25)	4.418 (6)	4.523 (11)	0.600 (42)	4.516 (10)	0.551 (23)	4.331	0.690
66	813353.587 (16)	4.256 (5)	4.332 (30)	0.512 (72)	4.326 (28)	0.577 (36)	4.106	0.652
69	849622.436 (16)	4.153 (5)	4.257 (11)	0.608 (37)	4.249 (11)	0.603 (27)	3.960	0.619

maximum around the value $J = 20$ corresponding to the so-called rotational resonance.[31,32] From the comparison of the various line shape models considered it appears that the SD-Voigt broadenings are quite similar for both models, but are larger than the Voigt broadenings, which agrees with the earlier observations. Moreover, one observes that this feature is more pronounced at very low J-values. Particularly and by contrast with the Voigt model, SD-Voigt broadenings exhibit a slight minimum for $J \approx 3$.

Since there is a close correspondence via Eq. (3) between both considered SD-Voigt models, only the J-dependence of the α parameter corresponding to the HG-SD-Voigt model has been drawn in Fig. 4 (lower panel). Except for the $J \rightarrow J' = 1 \rightarrow 2$ line for which a large α-value of about 1.3 was found one observes soft variations of α around 0.6. Within the Berman-Pickett model,[7,8] this would correspond to an effective potential in the form $V(r) \propto 1/r^q$ with $q \cong 6$.

In order to confirm the physical origin of departures from the Voigt profile, line fits have been attempted by using the Galatry profile.[16] Such fits were possible just for the highest frequency lines considered in this study and only at low pressures, when the collisional broadening is not much larger than the Doppler broadening. As an example, Fig. 5 presents the case of the $J \rightarrow J' = 58 \rightarrow 59$ line at 716.5 GHz at 0.602 Torr pressure. By using the Voigt profile, residuals display the usual signature of line narrowing. The Galatry and Q-SD-Voigt profiles are both well suited for reproducing the observed line shape to the noise level and lead to similar collisional relaxation rates $\Gamma_0/(2\pi)$ (2.879(4) and 2.897(4) MHz, respectively), larger than the Voigt one (2.835(3) MHz). However, it must be noted that for higher pressures, any fits using the Galatry profile failed, whereas no difficulties were encountered by using Q-SD-Voigt or HG-SD-Voigt profiles. Such a failure of the Galatry profile has already been described in earlier papers[13,25,34–36] and is well understood from the value of the retrieved optical diffusion rate $\beta_{opt}/(2\pi) = 3.34(45)$ MHz. Not only the estimated uncertainty is worse compared to those obtained for Q-SD- and HG-SD-Voigt parameters [$\Gamma_2/(2\pi) = 0.30(1)$ MHz and $\alpha = 0.57(2)$, respectively], but the retrieved $\beta_{opt}/(2\pi)$ value is nearly six times larger than the kinetic diffusion rate $\beta_{kin}/(2\pi) = 0.59$ MHz expected for OCS.[21,22] Such a result is physically meaningless because the optical diffusion rate cannot be larger than the kinetic diffusion rate. Indeed, for the considered pressure range, departures from the Voigt profile result mainly from the speed dependence of relaxation rates. Finally and without going into details, it has been shown in Ref. 13 that for collisional rates Γ_0 approaching or larger than a limiting value given within 10% by $\Gamma_0^{lim}/k v_{a0} \cong (\sqrt{3}\Gamma_2/\Gamma_0)^{-1}$, no fit can be performed by using the Galatry profile. In the case of the $J \rightarrow J' = 58 \rightarrow 59$ OCS line (see Table I) for which $\Gamma_2/\Gamma_0 = 0.150(5)$, this limit Γ_0^{lim} is 2.64 MHz, corresponding to

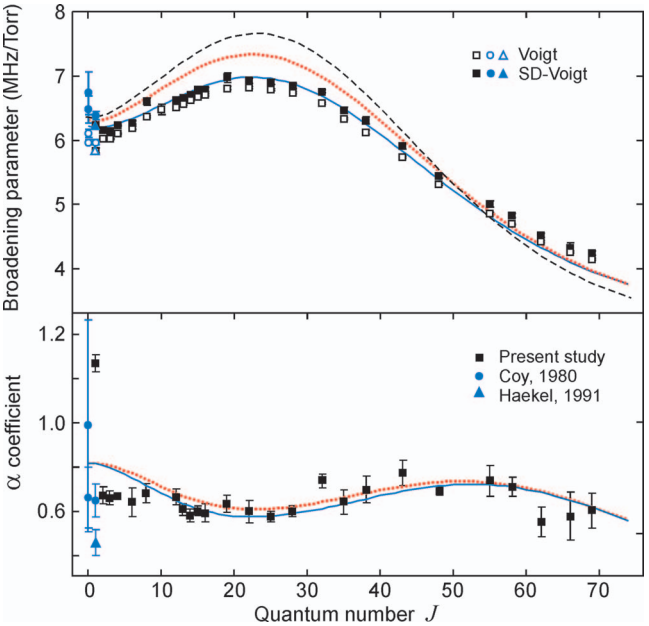

FIG. 4. OCS self-collisional relaxation at 296 K versus rotational quantum number J. Upper panel: broadening parameters γ_0 (in MHz/Torr). This work: Voigt (□); HG-SD-Voigt (■). Other works:[14,33] Voigt (○,△); SD-Voigt (●,▲). Dashed line: theoretical $\gamma(\bar{v}_r)$ values; dotted line: theoretical averaged γ_0 values; solid line: integration bounded to 18 Å in Eq. (6) (see text). Lower panel: SD-exponent α. This work (■); other works[14,33] (●,▲). Dotted line: theoretical α values; solid line: integration bounded to 18 Å in Eq. (6) (see text). For clarity, error bars correspond to three standard deviations.

the pressure of about 0.55 Torr, which is in agreement with our trials.

For the sake of completeness, similar fits have been performed using the Q-SD-Galatry profile.[19,37] In order to avoid fitting instabilities, the optical diffusion rate β_{opt} has to be fixed at some *a priori* value. According to the previous discussion, β_{opt} was conservatively set at the kinetic diffusion value $\beta_{\text{kin}} = 2\pi P \beta_{\text{kin}}{}^0$ with $\beta_{\text{kin}}{}^0 = 0.989$ MHz/Torr. The Q-SD-Galatry profile leads to retrieved γ_0 and γ_2 parameters lower than those derived from the Q-SD-Voigt profile by about 4 and

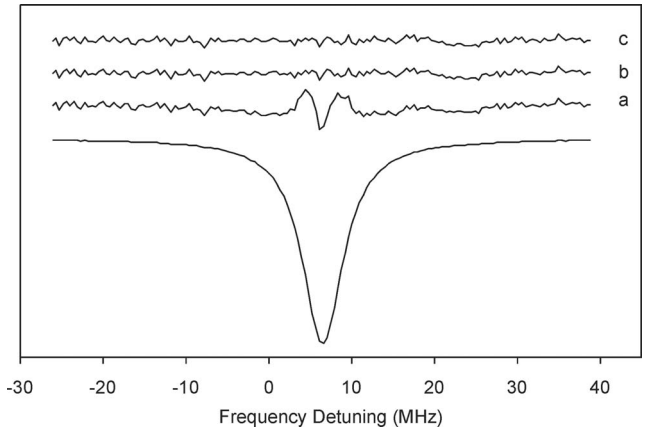

FIG. 5. $J \rightarrow J' = 58 \rightarrow 59$ line of OCS. Residuals (amplified by 20) correspond to Voigt (a), Galatry (b), and Q–SD–Voigt (c) profiles. Frequency detuning is shown from 716.540 GHz. Temperature: 297 K. Cell length: 1.5 cm. OCS pressure: 0.602 Torr. Doppler half-width at 1/e level: 0.686 MHz. Voigt collisional half-width: 2.835(3) MHz. Calculated peak relative absorption at infinite pressure: 8.1%.

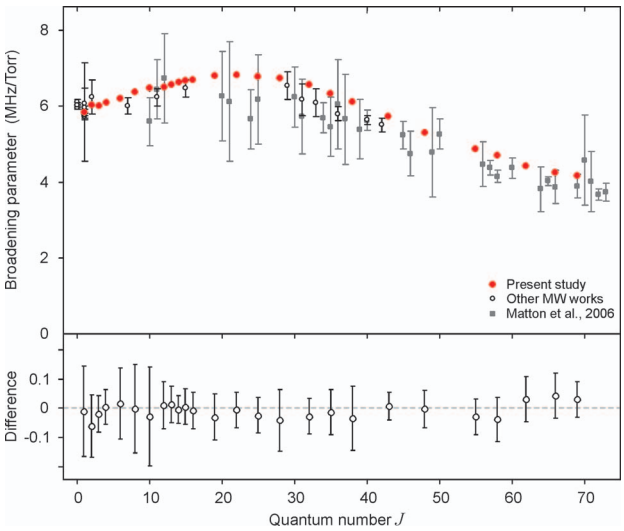

FIG. 6. Comparison of OCS self-relaxation parameters γ_0 (in MHz/Torr) at 296 K versus J obtained from different laboratories and by various techniques (upper panel). All results refer to the Voigt profile. Other MW works: Refs. 14, 33, 41, and 45; Matton *et al.*: Ref. 27. The lower panel presents the difference (in MHz/Torr) between results of Ref. 5 and the present work. Error bars correspond to three standard deviations. In the lower panel unified uncertainties of both data sets are shown.

10 kHz/Torr, respectively. The difference is only 0.5 of standard statistical deviation. So values of parameters are, in fact, in agreement within the estimated uncertainty. This confirms that the Dicke effect plays no role for the OCS-OCS system under our experimental conditions.

C. Comparison with other works

A number of works have been devoted to the self-collisional relaxation of OCS in the millimeter-submillimeter range. Results of the best known studies are presented in the upper panel of Fig. 6. Most of them were obtained by usual line shape measurements,[38–40] including the frequency modulation technique,[41] and photomixing experiments.[27] Interesting and accurate results were also obtained for the lowest J-values[42–44] and for some l-doublet lines[45] by using time domain experiments. The lower panel of Fig. 6 presents the differences on enlarged scales between the results of Ref. 5 and those obtained in this study from the Voigt model. This figure demonstrates that the different data treatment including, in particular, another approach to the baseline accounting, has not introduced any noticeable systematic deviation in the derived line parameters.

Finally, let us consider data from the pioneering experiments of Coy[14] as well as the more recent results of Haekel and Mäder[33] who succeeded in a clear experimental evidence of speed dependence effects on the $J \rightarrow J' = 0 \rightarrow 1$ and $1 \rightarrow 2$ OCS lines. Although they considered a linear model for the absorber speed dependence of relaxation rates, a comparison with the quadratic model or with the hypergeometric model via linearization of Eq. (2)[12] and Eq. (3) is possible. The corresponding broadening values, reported in Fig. 4 (upper panel), are in good agreement with our results within 2.5%, i.e., three standard deviations. However, a strong

difference is observed for the SD-parameter α related to the $J \rightarrow J' = 1 \rightarrow 2$ line; our results are at least twice larger than those deduced from experiments by Coy and Haekel. This discrepancy could be potentially attributed to specificity of our experimental setup. The dimensions of the used radio-acoustic cell become comparable with the radiation wavelength corresponding to this transition. In spite of all precautions undertaken, this may lead to a non-uniform distribution of radiation power inside the cell, intensifying the apparatus baseline problems. The discrepancy may also originate from the use for this particular line study of a radiation source with larger phase noises than for the other lines. Since the results of Coy and Haekel are in fine agreement with our observations dealing with higher J-values, we consider that the discrepancy originated from a possible artifact in our experiment.

D. Approximation of the experimental data

Accurate values of line shape parameters for each spectral line are compulsory for various spectroscopic applications. Since not all transitions of the spectrum were studied, we used a 4,4-Padé approximant as an empirical approach to obtain J-dependences of the line shape parameters. The approximation procedure was similar to the one described in Ref. 5. The following rational function was used:

$$f(J) = \frac{\sum_{i=0}^{4} a_i J^i}{1 + \sum_{i=1}^{4} b_i J^i}, \tag{5}$$

where f is either the collisional broadening parameter γ_0 or the SD-parameter α, a_i, and b_i are adjustable coefficients. The approximation was made for the results related to the HG-SD-Voigt model. The adjustable coefficients obtained from the fit are listed in Table II. The discrepancy between the experimental values and the fitting curve is within triple statistical uncertainty of the experimental data practically for all points for both dependences. The obtained set of parameters allows a good interpolation between measured data. Some cautious extrapolation of the broadening parameter is possible because for increasing J the approximant smoothly approaches the finite value of about 2.8 MHz/Torr. Concerning the SD-parameter α, the extrapolation gives diverging values, so just using the constant value $\alpha = 0.6$ is preferable. This should be quite sufficient for modeling the major part of the line shape departure from the Voigt profile.

TABLE II. Fitted coefficients of the 4,4-Pade approximant (Eq. (5)) for the self-broadening parameter γ_0 (in MHz/Torr) and the SD parameter α (dimensionless) of the OCS rotational spectrum lines.

Coefficient	γ_0	α
a_0	0.6943×10^{1}	0.6792×10^{0}
a_1	0.1225×10^{2}	-0.4206×10^{-1}
a_2	0.3735×10^{-1}	0.9062×10^{-3}
a_3	0	-0.5715×10^{-5}
a_4	0.6461×10^{-4}	0
b_1	0.2097×10^{1}	-0.5657×10^{-1}
b_2	-0.1653×10^{-1}	0.1098×10^{-2}
b_3	0	-0.5958×10^{-5}
b_4	0.2312×10^{-4}	0

IV. THEORETICAL CALCULATIONS

A. Principle of calculations

The collisional relaxation parameters of $^{16}O^{12}C^{32}S$ in collision with OCS in natural abundance are calculated on the basis of the RB formalism.[6] The calculations are similar to those reported in the ν_1 band of OCS.[46] Within the semiclassical frame, the relaxation parameter $\gamma_{if}(v_r)$ of an isolated $J_i \rightarrow J_f$ line may be expressed as a function of the relative molecular speed v_r such that

$$\gamma_{if}(v_r) = \frac{n\, v_r}{2\pi} \sum_{J_2} \rho(J_2) \int_0^{\infty} S_{if}(b, v_r, J_2) 2\pi\, b\, \mathrm{d}b, \tag{6}$$

where n is the number density of perturbing molecules; J_2 are the rotational quantum numbers for the perturber molecule, $\rho(J_2)$ is the relative population distribution in the $|J_2\rangle$ ground vibrational state of the perturber, S_{if} is the complex differential cross section representing the collisional efficiency, and b is the impact parameter. The imaginary part of S_{if} providing an essential contribution to line shifts (which were found, however, to be very weak) has no influence on the collisional relaxation parameter given with five digits and, therefore, can be omitted. Thus, the expression for the differential cross section is given by[47,48]

$$S_{if}(b, v_r, J_2) = 1 - \exp\left[-\sum_{\ell_1 \ell_2} \left({}^{\ell_1\ell_2}S_{2,i2} - {}^{\ell_1\ell_2}S_{2,f2} - {}^{\ell_1\ell_2}S_{2,f2i2} \right) \right], \tag{7}$$

where $S_{2,i2}$, $S_{2,f2}$, and $S_{2,f2i2}$ are second-order terms of the perturbation development of S_{if} derived from the anisotropic part of the potential,[6] ℓ_1 and ℓ_2 represent the order of the spherical harmonics for the absorber and the perturber: 1 for $|\Delta J| = 1$ (dipolar transition), 2 for $|\Delta J| = 0, 2$ (quadrupolar transition), 3 for $|\Delta J| = 1, 3$ (octopolar transition).

For the description of the trajectories where long range forces dominate, we used an equivalent straight path trajectory[49] around the distance of closest approach r_c, calculated from the isotropic part of the potential, taken as a 6–12 Lennard-Jones potential.

Relaxation parameters at 296 K have been computed for rotational lines of OCS by including the contributions of the perturber in the ground state with J_2 values up to 100, which takes into account about 99% of the absorber collisional partners. As for other polar molecules, the electrostatic interaction V_e makes a dominant contribution to the self-broadening. Therefore the anisotropic potential used in the calculations has been generally limited to this interaction to which we have added a dispersion contribution V_{SGC} derived from the potential first considered by Smith, Giraud,

and Cooper[50] according to

$$V_{\text{aniso}} = V_{\text{e}} + V_{\text{SGC}} \tag{8a}$$

with[47]

$$V_{\text{e}} = V_{\mu_1\mu_2} + V_{\mu_1 Q_2} + V_{\mu_2 Q_1} + V_{Q_1 Q_2} + V_{\mu_1\Omega_2} + V_{\mu_2\Omega_1} + V_{Q_1\Omega_2} + V_{Q_2\Omega_1} + V_{\Omega_1\Omega_2}, \tag{8b}$$

where the indices 1 and 2 refer to the absorber and the perturber, μ, Q, and Ω are the dipole, quadrupole, and octopole moments of OCS, and

$$V_{\text{SGC}} = -4\varepsilon\left[A_1\left(\frac{\sigma}{r}\right)^7 P_1(\cos\theta) + A_2\left(\frac{\sigma}{r}\right)^6 P_2(\cos\theta)\right]. \tag{8c}$$

Here ε and σ are the depth and radius of the Lennard-Jones potential, A_1 and A_2 are adjustable effective parameters, P_1 and P_2 are first- and second-order Legendre polynomials and θ is the angle between the absorber axis and the intermolecular axis. However, several aspects of the potential used must be pointed out:

The short-range interactions in $R_1(\sigma/r)^{12}$ and $R_2(\sigma/r)^{12}$ of V_{SGC}[50] provide a negligible contribution even at high J-values and have not been considered in this study. Note moreover that the same angular dependence assumed for the attractive and repulsive parts of this potential leads to negative cross-term contributions from A_1R_1 and A_2R_2 [51] which have a comparable influence in second-order terms S_2 to the positive contributions from ${R_1}^2$ and ${R_2}^2$.

The r^{-6} term of V_{SGC} implicitly includes an induction contribution. This contribution has been estimated through the formalism developed by Leavitt (the first two terms in Eq. D10a of Ref. 47) and was found to be much weaker than the dispersion contribution and indeed almost negligible.

The dispersion contributions are only significant at low J-values ($J < 10$) and it is very difficult to determine parameters A_1 and A_2 by adjusting the calculated broadening coefficients to the experimental data, as the single electrostatic potential V_{e} provides overestimated results for J-values around 20. Hence, we have used in the calculations the parameter values $A_1 = A_2 = 0.20$ fitted for OCS-Ar, OCS-N_2, and OCS-O_2.[51] Note also that the parameter A_1 is related to the separation between the mass and the charge centers of the active molecule, whereas A_2 is often taken as the reduced polarizability anisotropy of this molecule.[32,52] Therefore, the parameters A_1 and A_2 do not depend to the first approximation on the perturber, as was shown in Ref. 51 for the perturbers Ar, N_2, and O_2.

Since to our knowledge no data are available for the octopole moment of OCS, it was decided to use the plausible value $\Omega = 4$ DÅ^2 as in Ref. 51.

The rotational parameters, the multipole moments of OCS and the Lennard-Jones potential parameters ε and σ used in the calculations are listed in Table III. It should be noted that these values were all taken from the literature and were not adjusted to fit the experimental results.

TABLE III. Parameters used in the calculation of self-broadening in the rotational band of $^{16}O^{12}C^{32}S$.

B (GHz)[53]	D (kHz)[53]	μ (D)[54]	Q (DÅ)[55]	Ω (DÅ^2)[51]	ε (K)[56]	σ (Å)[56]
6.081492110	1.301387	0.71519	−0.786	4	286.9	4.099

B. Averaged relaxation parameters

As a first step and following Anderson's suggestion,[57] we have computed the relaxation parameter $\gamma(\bar{v}_r)$ related to the mean relative speed (MRS) $\bar{v}_r$. For comparison, several potentials have been considered. The corresponding results are displayed in Fig. 7 along with our experimental results.

In the case of electrostatic interactions given by Eq. (8b), the general behavior of experimental results is well reproduced with a maximum corresponding to most populated J-values, i.e., to the already mentioned rotational resonance condition.[32] Starting from the sole dipole-dipole interaction, the additional consideration of quadrupolar contribution leads to larger broadening values, this effect being more important at larger J-values. In a further calculation, we have also considered higher-order electrostatic contributions involving the octopole moment. These contributions yield slightly larger broadening coefficients, thus improving agreement with the experimental data at high J-values. This feature corresponds to the fact that, since dipole-dipole and dipole-quadrupole interactions get smaller for high J rotational lines, relaxation takes place for shorter intermolecular distances. Then the relative contributions from the octopole moment occurring for close collisions are intensified at high J, especially those derived from the dipole-octopole interaction giving a maximum efficiency for $J_{\text{i}} \approx 3J_{2\text{max}}$, where $J_{2\text{max}} = 22$ is the most populated level of the perturber at 296 K.[32] Finally, the dispersion and induction V_{SGC} potential defined by Eq. (8c) has been considered as well. Its contribution, quite small for middle and high J-values, is clearly significant at low J-values. Particularly, this extra contribution is responsible for a local minimum for $J \approx 2$–3. That characteristic, not deduced from

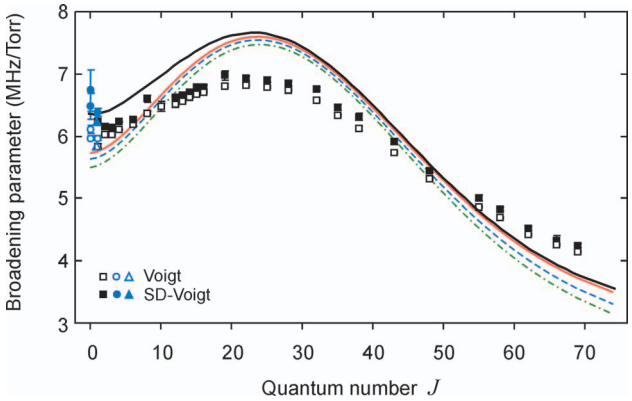

FIG. 7. OCS self-collisional relaxation at 296 K versus rotational quantum number J. See Fig. 4 for experimental points notations. Theoretical $\gamma(\bar{v}_r)$ values for various interaction models (see text): dipole (green dash-dotted line); dipole + quadrupole (blue dashed line); dipole + quadrupole + octopole (thin red solid line); dipole + quadrupole + octopole + SGC (thick black solid line).

the sole consideration of electrostatic interactions (Eq. (8b)), is specific for the V_{SGC} contribution. It is in full agreement with the experimental features already mentioned for the SD-Voigt results and not observed when the Voigt model is used (see Sec. III B). So, on the one hand, the general trend of the relaxation J-dependence is better reproduced and results are satisfactory for low J-values, which suggests that the retained A_1 and A_2 values are quite reasonable. On the other hand, such an agreement demonstrates that a reliable interpretation of collisional broadening experiments requires not only a realistic line shape model, but an accurate theoretical model as well.

As those obtained in the ν_1 band,[46] the theoretical results remain notably greater than the experimental data for middle J-values for which the broadenings are the largest and are underestimated at large J-values ($J > 60$). Then, as a second step, we have considered the speed averaged broadening parameters γ_0 defined as

$$\gamma_0 = \langle \gamma(v_r) \rangle = \int_0^\infty \gamma(v_r) f(v_r) \mathrm{d}v_r, \tag{9}$$

where $f(v_r)$ is the Maxwell distribution of relative speeds (DRS). Equation (6) was computed by using about 70 v_r values ranging from 0 to 4 times the most probable relative speed. Following the method described in Ref. 58, care was taken to discard any contribution of orbiting collisions corresponding to bound translational states. As can be seen in Fig. 4 (upper panel), the consideration of the Maxwell-Boltzmann speed distribution leads to a decrease of calculated results for J in the range 15–30 and some increase at high J-values, giving better agreement with the experimental data. This confirms the conclusions emphasizing the importance of Maxwell-Boltzmann speed averaging in theoretical calculations.[59,60]

However, these theoretical results, even the ones derived from DRS, remain significantly larger than the experimental ones for the largest broadenings. This discrepancy is not surprising since for molecules with strong dipole and/or quadrupole moments, such as CO_2,[61] CH_3Cl,[62] CH_3F,[63] or CH_3Br,[64] the self-broadening coefficients calculated from the most accurate values of electric moments are generally overestimated. The disagreement between calculations and measurements probably arises from the great interaction distances ($r > 50$ Å) in the integral of Eq. (6) because of the strong dipole-dipole and dipole-quadrupole contributions to $S_2(b)$.[65] To obtain better agreement between the theoretical results derived from DRS and the experimental values, we have calculated the integral over the impact parameter b from 0 to an arbitrary limit b_{lim} instead of the infinite one. An empirical b_{lim} value, equal to 18 Å, leads to satisfactory agreement between calculated and experimental data (Fig. 4, upper panel). It can be seen that these differences between both sets of calculated results negligible at high J-values are greater for middle J-values where the broadenings are the largest, corresponding to the resonance condition[32] for the predominant dipole-dipole interaction. Theoretical γ_0 values corresponding to this empirical limitation of the upper bound of the integral of Eq. (6) with $b_{\mathrm{lim}} = 18$ Å case are reported in Table I.

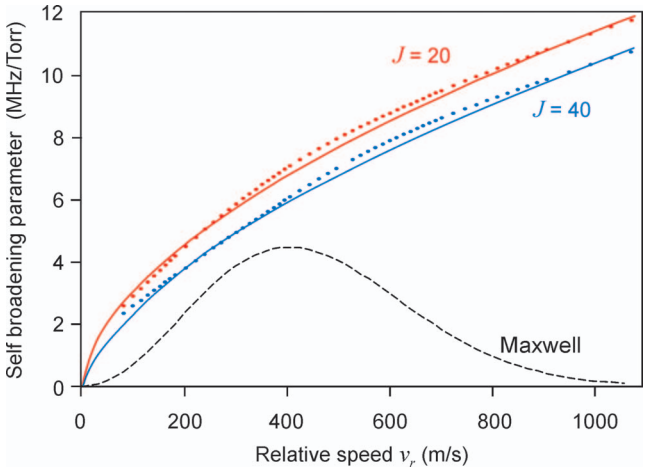

FIG. 8. Self-broadening parameters $\gamma(v_r)$ of OCS versus the relative speed v_r at 296 K for two $J \rightarrow J'$ transitions. Dots correspond to values computed from Eq. (6) with dipole + quadrupole + octopole + SGC contributions. Solid lines result from fit of Eq. (10) to computed points. The dashed line is the Maxwell distribution of relative speeds.

It should be pointed out that the resulting theoretical calculations are in a much better agreement with the experimental results obtained from the SD-Voigt profiles than with those corresponding to the Voigt profile. This also reveals drawbacks of the Voigt model that neglects the correlation between frequency of collisions and molecular velocities and considers the collisional broadening γ_0 as an *ad hoc* parameter. On the contrary, SD-Voigt profiles refer to a realistic analysis of collisional processes. Moreover, speed dependent models contain a broadening parameter γ_0 that corresponds to a physically grounded definition given by Eq. (9).

C. Speed dependence of collisional relaxation

The speed dependence of collisional relaxation has been computed from Eq. (6) and using the potential defined by Eq. (8a) that includes electrostatic and dispersion contributions. Corresponding $\gamma(v_r)$ values have been modeled according to the Berman-Pickett model[7–10] written as

$$\gamma(v_r) = \gamma(\bar{v}_r) \left(\frac{v_r}{\bar{v}_r}\right)^\alpha = \left(\frac{\sqrt{\pi}}{2}\right)^{1-\alpha} \frac{\gamma_0}{\Gamma_{\mathrm{funct}}\left(\frac{3+\alpha}{2}\right)} \left(\frac{v_r}{\bar{v}_r}\right)^\alpha, \tag{10}$$

where $\Gamma_{\mathrm{funct}}(x)$ is Gamma function[11] and $\bar{v}_r$ is mean relative speed. Theoretical values of the speed dependent parameter α have been retrieved from the $\gamma(v_r)$ values by using a least-squares fit procedure weighted by the Maxwell-Boltzmann distribution of speeds. Let us note that γ_0 values have been derived using Eq. (9) and they have been fixed in this fit.

Figure 8 displays a typical behavior of $\gamma(v_r)$ versus relative speed as well as the curve fitted according to Eq. (10) calculated for two J-values in the particular case $b_{\mathrm{lim}} = 18$ Å chosen because it fairly reproduces observed γ_0 broadening values (see Sec. IV B). This figure demonstrates a good qualitative agreement of the calculated values with the model described by Eq. (10) for the most significant part of

the Maxwell distribution of speeds. For the sake of comparison, both limit values of b_{lim}, i.e., infinity and 18 Å have been considered and the corresponding theoretical SD-coefficients α are displayed in Fig. 4 (lower panel) along with the experimental results. On account of the moderate accuracy achieved for this parameter, both calculations lead to very similar results that clearly reproduce the dependence of α on J-values deduced from our frequency domain experiments as well as from those of Coy[14] and Haekel[33] performed in the time domain. This α parameter has a minimum ($\cong 0.6$) for J around 20 and a maximum ($\cong 0.75$) for J around 50. The theoretical values of the parameters corresponding to the aforementioned empirical limitation with $b_{\text{lim}} = 18$ Å are reported in Table I.

V. CONCLUSION

The $^{16}O^{12}C^{32}S$ rotational line profiles experimentally observed with a high signal to noise ratio at room temperature and at pressures when collisional broadening considerably prevails over the Doppler line width have been analyzed. The analysis demonstrates that the data cannot be reproduced to the noise level by the traditional Voigt profile because this model assumes independence of collisional and Doppler broadenings. On the one hand, the theoretical models taking into account the correlation between these two line broadening mechanisms allow not only perfect fit of the experimental data but also derivation of reasonable parameters of the speed dependence of collisional relaxation. On the other hand, strong failures of the models accounting only for the Dicke effect have been observed, which rules out any significant influence of velocity changing collisions for OCS. These conclusions are similar to those already obtained in various spectral ranges for many molecules of atmospheric interest. For the first time they are validated for nearly the whole rotational spectrum. Refined values of collisional self-broadening coefficients as well as new information on speed dependence parameters are obtained and compared with the previously known data.

The self-broadening coefficients of pure rotational transitions of OCS have been calculated and compared with experimental measurements. The calculations have been performed from the semiclassical Robert-Bonamy model involving the main electrostatic interactions and a dispersive anisotropic potential. This model reproduces fairly well the general behavior of relaxation parameters as a function of the rotational quantum number *J*. The dispersive interaction contribution at low *J*-values has been emphasized particularly because it leads to a better qualitative agreement with SD-Voigt results than with pure Voigt ones. From a quantitative point of view, a significant improvement is obtained by using in calculations the Maxwell-Boltzmann distribution of relative molecular speeds instead of the mean relative speed. However, as it often occurs for strongly polar molecules, the calculations overestimate the broadening coefficients. Satisfactory agreement with measurements was achieved by arbitrarily limiting the upper bound of integration of the differential cross section to the impact parameter of 18 Å. The theoretically calculated speed dependence parameters, with or without this empirical limitation, are in a good agreement with the experimentally obtained values.

Thus, analysis of experimental data as well as theoretical calculations performed in this work confirm the importance of taking the speed dependence of collisional interaction into account, if highly accurate and physically grounded information on molecular absorption is required. This study also confirms the previously made conclusions that the speed dependent Voigt profile should be used instead of the traditional Voigt profile as the actual line shape model.

ACKNOWLEDGMENTS

The work was partly supported by the Russian Foundation for Basic Research. The Laboratoire de Physique des Lasers, Atomes et Molécules belongs to the Centre d'Etudes et de Recherches Lasers et Applications (CERLA) and by the Région Nord-Pas de Calais and the Fonds Européen de Développement Economique des Régions (FEDER).

[1] J. J. Harrison, P. F. Bernath, and G. Kirchengast, J. Quant. Spectrosc. Radiat. Transf. **112**, 2347 (2011).
[2] J.-M. Hartmann, C. Boulet, and D. Robert, *Collisional Effects on Molecular Spectra. Laboratory Experiments and Models, Consequences for Applications* (Elsevier, Amsterdam, 2008).
[3] F. Rohart, AIP Conf. Proc. **1058**, 94 (2008).
[4] M. Yu. Tretyakov, M. A. Koshelev, D. S. Makarov, and M. V. Tonkov, Instrum. Exp. Tech. **51**, 78 (2008).
[5] M. A. Koshelev and M. Yu. Tretyakov, J. Quant. Spectrosc. Radiat. Transf. **110**, 118 (2009).
[6] D. Robert and J. Bonamy, J. Phys. (Paris) **40**, 923 (1979).
[7] P. R. Berman, J. Quant. Spectrosc. Radiat. Transf. **12**, 1331 (1972).
[8] H. M. Pickett, J. Chem. Phys. **73**, 6090 (1980).
[9] M. Findeisen, T. Grycuk, A. Bielski, and J. Szudy, J. Phys. B **20**, 5597 (1987).
[10] F. Rohart, L. Nguyen, J. Buldyreva, J.-M. Colmont, and G. Wlodarczak, J. Mol. Spectrosc. **246**, 213 (2007).
[11] M. Abramowitz and I. A. Stegun, *Handbook of Mathematical Functions* (Dover, New York, 1965).
[12] F. Rohart, H. Mäder, and H.-W. Nicolaisen, J. Chem. Phys. **101**, 6475 (1994).
[13] J.-F. D'Eu, B. Lemoine, and F. Rohart, J. Mol. Spectrosc. **212**, 96 (2002).
[14] S. L. Coy, J. Chem. Phys. **73**, 5531 (1980); **76**, 2112 (1982).
[15] R. H. Dicke, Phys. Rev. **89**, 472 (1953).
[16] L. Galatry, Phys. Rev. **122**, 1218 (1961).
[17] S. C. Rautian and I. I. Sobel'man, Usp. Fiz. Nauk **90** 209 (1966) [Sov. Phys. Usp. **9**, 701 (1967)].
[18] P. Duggan, P. M. Sinclair, M. P. Le Flohic, J. W. Forsman, R. Berman, A. D. May, and J. R. Drummond, Phys Rev. A **83**, 2077 (1993).
[19] R. Ciuryło and J. Szudy, J. Quant. Spectrosc. Radiat. Transf. **57**, 411 (1997).
[20] M. D. De Vizia, F. Rohart, A. Castrillo, E. Fasci, L. Moretti, and L. Gianfrani. Phys. Rev. A **83**, 052506 (2011).
[21] J. O. Hirschfelder, C. F. Curtis, and R. B. Bird, *Molecular Theory of Gases and Liquids* (Wiley, New York, 1964).
[22] A. Henry, D. Hurtmans, M. Margotin-Maclou, and A. Valentin, J. Quant. Spectrosc. Radiat. Transf. **56**, 647 (1996).
[23] J. P. Looney, Ph.D. dissertation, Pennsylvania State University, Philadelphia, 1987.
[24] J. M. Colmont, J.-F. D'Eu, F. Rohart, G. Wlodarczak, and J. Buldyreva, J. Mol. Spectrosc. **208**, 197 (2001).
[25] H. Tran, D. Bermejo, J.-L. Domenech, P. Joubert, R. R. Gamache, and J.-M. Hartmann, J. Quant. Spectrosc. Radiat. Transf. **108**, 126 (2007).
[26] I. I. Sobel'man, *Introduction to the Theory of Atomic Spectra* (Pergamon, Oxford, 1972).
[27] S. Matton, F. Rohart, R. Bocquet, G. Mouret, D. Bigourd, A. Cuisset, and F. Hindle, J. Mol. Spectosc. **239**, 182 (2006).
[28] G. Birnbaum, Adv. Chem. Phys. **12**, 487 (1967).

[29]J.-P. Bouanich and G. Blanquet, J. Quant. Spectrosc. Radiat. Transf. **40** 205 (1988).
[30]G. Yu. Golubiatnikov, A. V. Lapinov, A. Guarnieri, and R. Knöchel, J. Mol. Spectrosc. **234**(1), 190–194 (2005).
[31]C. H. Townes and A. L. Schawlow, *Microwave Spectroscopy* (McGraw-Hill, New York, 1955).
[32]M. Giraud, D. Robert, and L. Galatry, J. Chem. Phys. **53**, 352 (1970); C. R. Acad. Sci. (Paris) **272**, 1252 (1971).
[33]J. Haekel and H. Mäder, J. Quant. Spectrosc. Radiat. Transf. **46**, 21 (1991).
[34]R. Wehr, R. Ciuryło, A. Vitcu, F. Thibault, J. R. Drummond, and A. D. May, J. Mol. Spectrosc. **235**, 54 (2006).
[35]F. Rohart, G. Wlodarczak, J.-M. Colmont, G. Cazzoli, L. Dore, and C. Puzzarini. J. Mol. Spectrosc. **251**, 282 (2008).
[36]A. Predoi-Cross, F. Rohart, J.-P. Bouanich, and D. R. Hurtmans, Can. J. Phys. **87**, 485 (2009).
[37]D. Priem, F. Rohart, J.-M. Colmont, G. Wlodarczak, and J.-P. Bouanich, J. Mol. Struct. **517–518**, 435 (2000).
[38]D. S. Olson, C. O. Britt, V. Prakash, and J. E. Boggs, J. Phys. B **6**, 206 (1973).
[39]R. P. Leavitt and J. P. Slattler, J. Quant. Spectrosc. Radiat. Transf. **29**, 179 (1983).
[40]B. Lamalle, P. Suzeau, F. Truchetet, and J. Chanussot, Can. J. Phys. **65**, 452 (1987).
[41]G. Cazzoli and L. Dore, J. Mol. Spectrosc. **141**, 49 (1990).
[42]J. C. McGurk, H. Mäder, R. T. Hofmann, T. G. Schmalz, and W. H. Flygare, J. Chem. Phys. **61**, 3759 (1974).
[43]S. L. Coy, J. Chem. Phys. **63**, 5145 (1975).
[44]H. Bomsdorf, H. Dreizler, and H. Mäder, Z. Naturforsch. **35a**, 723 (1980).
[45]S. C. Mehrotra and H. Mäder, Can. J. Phys. **62**, 1280 (1984).
[46]J. P. Bouanich, G. Blanquet, J. Walrand, and C. P. Courtoy, J. Quant. Spectrosc. Radiat. Transf. **36**, 295 (1986).
[47]R. P. Leavitt, J. Chem. Phys. **73**, 5432 (1980).
[48]R. P. Leavitt and D. Korff, J. Chem. Phys. **74**, 2180 (1981).
[49]J. Bonamy, L. Bonamy, and D. Robert, J. Chem. Phys. **67**, 4441 (1977).
[50]E. W. Smith, M. Giraud, and J. Cooper, J. Chem. Phys. **65**, 1256 (1976).
[51]J. L. Domenech, D. Bermejo, and J.-P. Bouanich, J. Mol. Spectrosc. **200**, 266 (2000).
[52]R. H. Tipping and R. M. Herman, J. Quant. Spectrosc. Radiat. Transf. **10**, 881 (1970).
[53]S. Saupe, M. H. Wappelhorst, B. Meyer, W. Urban, and A. G. Maki, J. Mol. Spectrosc. **175**, 190 (1996).
[54]L. S. Masukidi, J. G. Lahaye, and A. Fayt, J. Mol. Spectrosc. **148**, 281 (1991).
[55]F. H. de Leeuw and A. Dymanus, Chem. Phys. Lett. **7**, 288 (1970).
[56]S. V. Churakov and M. Gottschalk, Geochim. Cosmochim. Acta **67**, 2397 (2001).
[57]P. W. Anderson, Phys. Rev. **76**, 647 (1949).
[58]J. P. Looney and R. M. Herman, J. Quant. Spectrosc. Radiat. Transf. **37**, 547 (1987).
[59]R. R. Gamache and L. Rosenmann, J. Mol. Spectrosc. **164**, 489 (1994).
[60]R. R. Gamache, J. Mol. Spectrosc. **208**, 79 (2001).
[61]L. Rosenmann, J. M. Hartmann, M. Y. Perrin, and J. Taine, J. Chem. Phys. **88**, 2999 (1988).
[62]G. Blanquet, J. Walrand, J. C. Populaire, and J. P. Bouanich, J. Quant. Spectrosc. Radiat. Transf. **53**, 211 (1995).
[63]B. Lance, M. Lepère, G. Blanquet, J. Walrand, and J.-P. Bouanich, J. Mol. Spectrosc. **180**, 100 (1996).
[64]L. Gomez, D. Jacquemart, J.-P. Bouanich, Z. Boussetta, and H. Aroui, J. Quant. Spectrosc. Radiat. Transf. **111**, 1252 (2010).
[65]C. Lerot, G. Blanquet, J.-P. Bouanich, J. Walrand, and M. Lepere, J. Mol. Spectrosc. **230**, 153 (2005).